Ion−Oligomer Interactions in Poly(ethylene glycol)400/$(LiCl)_x$ Electrolyte Complexes

Vito Di Noto,* Daniela Longo, and Vera Münchow

Dipartimento di Chimica Inorganica, Metallorganica ed Analitica dell'Università degli Studi di Padova, Via Loredan 4, I-35131 Padova, Italy

Received: September 17, 1998; In Final Form: December 31, 1998

By reacting metallic lithium with 1-chlorobutane we obtained a very anhydrous LiCl that allowed us to prepare 10 poly(ethylene glycol)/$(LiCl)_x$ complexes ($0 \leq x \leq 1.40665$) using a reaction protocol that does not require added solvents. The interactions between Li^+ and Cl^- ions and poly(ethylene glycol) (PEG) ligands in the polymer electrolytes were investigated by mid and far FT-IR spectroscopy. Results revealed that (a) the PEG chains assume a TGT type conformation; (b) Li^+ ions are coordinated by ethereal oxygens of the PEG ligand; (c) at an Li/O molar ratio less than 0.036, Cl^- ions form hydrogen bonding cages with the terminal OH groups of PEG chains; (d) at an Li/O molar ratio greater than 0.036, Cl^- ions are present both in hydrogen bonds and as "free anions" along PEG chains. Conductivity measurements made at different temperatures showed that these systems conduct ionically, with two distinct conductivity regions detected. The possible correlation between the conductivity and the structure of these electrolytic systems was also investigated showing that the "free ionic carriers", which are responsible for the A_σ values, are directly related to the total "free anion" concentration. The conductivity of PEG 400/$(LiCl)_{0.349}$ is on the order of $\simeq 1 \times 10^{-4}$ S cm^{-1} at 25 °C.

Introduction

In the past decade, various electrolyte polymers have been prepared and studied in many laboratories.[1,2] A recent book edited by Scrosati[3] presents applications of electrolyte polymers in the production of batteries and points out the tremendous potential technical applications of electrochemical energy storage systems based on these materials. Nonaqueous thin films of polymer electrolytes offer the following practical advantages: (a) low manufacturing cost and high performance; (b) economy of volume and mass; (c) structural and chemical stability; and (d) low toxicity.[4−6] All these features make polymer electrolytes very promising for the development of computers, communication devices, electric vehicles, industrial controls, toys, portable instruments, etc.

Such materials are currently obtained by doping an etheric oligomer or polymer with an inorganic salt. The most common method to prepare the polymer electrolytes is to dissolve or suspend both the salt and the host polymer in a common organic solvent such as acetonitrile and methanol, followed by removal of the solvent. Numerous studies have been carried out using alkaline metal salts, alkaline earth, and other divalent and trivalent metal salts[7−11] to understand the chemistry of the poly ether−inorganic salt complexation and to comprehend the mechanism of ionic conductivity of these systems, with the practical goal of increasing their conductivity. However, the transport properties of the produced electrolyte materials may vary with the choice of solvent.[12] On the other hand, as Ratner and Shriver[12] reported, for a given polymer host, a fairly sharp demarcation line may be established between salts that can and cannot form electrolytic complexes. These authors pointed out that those salts that are unable to form complexes simply have large lattice energies, which for lithium salts decreases in the order $F^- > Cl^- > Br^- > I^- > SCN^- > CF_3SO_3^-$. Thus, new inorganic lithium salts such as $LiN(CF_3SO_2)_2$ have been synthesized and proposed to prepare both liquid and solid polymer electrolytes.[13] Recently, a new salt was obtained by reacting powdered metallic magnesium with 1-chlorobutane.[14] This procedure yields a δ-$MgCl_2$ form that is extremely anhydrous and exhibits a much less crystallographic order compared to activated products obtained by rigorous purification of commercial starting materials. This chloride salt has a low lattice energy and is easily dissolved in PEG 400 without the need for organic solvents. The liquid polymer electrolyte thus obtained shows high ionic conductivity even at room temperature. Numerous studies have been carried out to understand the complicated nature of ionic conductivity and the complexation processes of cations and anions in the polymer host.[1,8] Several investigators[1,8−10,12,15,16] suggested that segmental motions of polymer host appear to be largely responsible for the ionic transport mechanism in the polymer electrolytic complexes. Furthermore, in recent studies it was proposed that ionic conductivity occurs through a charge hopping mechanism between adjacent sites having equivalent coordination symmetries,[9,10,14,17−19] and that this hopping process happens in two ways.[14,17−19] The first type of hopping event involves hopping between sites of the same polymer chain, i.e., *intrachain hopping* (intra-CH), and the second type occurs between different chains, i.e., *interchain hopping* (inter-CH).

In this paper we report the synthesis of a new anhydrous LiCl salt that is highly reactive toward coordinating agents. Direct dissolution of this product in poly(ethylene glycol) with a molecular weight of 400 (PEG 400) resulted in the formation of a series of PEG 400/$(LiCl)_x$ electrolytic complexes, with $0 \leq x \leq 1.40665$. The availability of these very pure electrolytic systems allowed us to carry out detailed investigations of Li^+−PEG and Cl^-−PEG interactions by FT-IR spectroscopy and to elucidate the inter-CH and the intra-CH conductivity mechanism

* Author to whom correspondence should be addressed. E-mail: dinoto@ux1.unipd.it. Fax: +39 49 8275161.

10.1021/jp983764y CCC: $18.00
Published on Web 03/18/1999

TABLE 1: Microanalytical Data for PEG 400/$(LiCl)_x$ Complexes with $0 \leq x \leq 1.306\,65$[a]

compd	Li (%)	PEG (%)	n_{Li} (mol)	n_{PEG} (mol)	$x = n_{Li}/n_{PEG}$	$r = n_{Li}/n_O$
1	0.0036	99.9964	5.186×10^{-4}	0.249 99	0.002 074	0.000 21
2	0.0158	99.9842	2.276×10^{-3}	0.249 96	0.009 105	0.000 94
3	0.0363	99.9677	4.653×10^{-3}	0.249 919	0.018 618	0.001 93
4	0.0634	99.9366	0.009134	0.249 841	0.036 56	0.003 78
5	0.1334	99.8666	0.01922	0.249 667	0.076 98	0.007 96
6	0.2680	99.732	0.03861	0.249 33	0.154 855	0.016 01
7	0.6021	99.3979	0.08674	0.248 495	0.349 06	0.036 10
8	1.1940	98.806	0.17202	0.247 015	0.696 39	0.072 02
9	2.3827	97.6173	0.34328	0.244 04	1.406 65	0.145 47

[a] n_{Li}, n_{PEG} and n_O are the moles of Li, PEG, and oxygen, respectively, in complexes.

in these complexes. The conductivity of PEG 400/$(LiCl)_x$ was also investigated at different temperatures and compositions.

Experimental Section

Reagents. Metallic lithium powder (≈325 mesh, 99.9%), 1-chlorobutane, PEG 400, and solvents were Aldrich reagent grade.

The reagents were further purified by standard methods, except for metallic lithium powder, which was utilized in the form supplied by the manufacturer. PEG 400 was dehydrated under high vacuum and at 90 °C. At first a vacuum of 10^{-3} mbar was used for 72 h and then 10^{-6} mbar for 48 h. The complete dehydration of PEG 400 was confirmed by Karl Fisher titration method. All reagents were stored under argon on 4A molecular sieves to prevent contamination by moisture. All transfer and handling operations were performed in a strictly argon atmosphere.

Synthesis of LiCl. Anhydrous 1-chlorobutane (400 mL) was added to 2.29 g of powdered lithium in a strictly argon atmosphere. The mixture was refluxed at the boiling temperature until complete reaction of the metallic lithium. The resulting thick white-violet solid was separated, carefully washed four times with *n*-heptane and then dried for 1 day at 140 °C under vacuum (10^{-3} mbar). Elemental analyses showed that the product contains low trace amounts of C and H; N and S are absent. The composition of Li salt consists of 83.20% Cl and 16.28% Li. Li was determined by inductively coupled plasma atomic emission spectroscopy (ICP-AES) after dissolution of the sample in bidistilled water and Cl by Mohr titration; results evidenced that LiCl represents 99.45% of the solid product, with other lithium metallorganic species accounting for the remaining ca. 0.55%.

Preparation of PEG 400/$(LiCl)_x$ Complexes. LiCl (7.71 g) was gradually added to 75 mL of PEG 400 in a 100 mL flask. The mixture was heated to 80 °C and stirred for 2 h; the LiCl was easily and completely dissolved. After cooling to room temperature a reddish, transparent, homogeneous and very viscous liquid was obtained. Ten PEG 400/$(LiCl)_x$ complexes with $0 \leq x \leq 1.40665$ were obtained by diluting this mother solution with PEG 400. The exact salt concentration in the polymer electrolytes was determined by dissolving the samples in bidistilled water and analyzing Li concentration by the method of standard additions and ICP-AES spectrometry.

Analytical data are reported in Table 1.

Instrumentation. ICP-AES measurements were carried out using a Spectroflame Modula sequential and simultaneous spectrometer equipped with a capillary cross-flow nebulizer (Spectro Analytical, Kleve, Germany). Li determinations were performed using a plasma power of 1.2 kW, a radio frequency generator of 27.12 MHz, and an argon gas flow with nebulizer, auxiliary, and coolant controls set at 1, 0.5, and 14 L/min, respectively. The lithium emission line was set at 670.784 nm and the argon reference line at 430.01 nm.

X-ray diffraction (XRD) patterns were scanned using the transmission technique with a GD-2000 diffractometer (Ital Structures, Riva del Garda, Italy), operating in the Seeman-Bohlin geometry and equipped with a quartz curved-crystal monochromator of the Johansson type aligned on the primary beam. Cu Kα1 radiation ($\lambda = 1.5406$ Å) was employed, and an instrumental 2θ step of 0.1° every 10 s was selected.

FT-IR spectra in the mid-infrared (MIR) and far-infrared (FIR) were recorded using a Nicolet 5SxC spectrometer equipped with a triglycine sulfate (TGS) detector, at a nominal resolution of 2 cm^{-1} and collecting 900 scans. The Happ−Genzel apodization method was adopted.[20] The samples were prepared under an argon atmosphere in cells equipped with KBr and polyethylene windows for measurements in the MIR and far-IR region, respectively.

Ac impedance measurements were carried out between the frequencies of 20 Hz and 1 MHz using a computer-controlled HP 4284A precision LCR meter. The data were collected by placing the samples between two parallel platinum blocking electrodes using a Amel model 192 conductivity cell with a constant of 0.985 cm. The determinations were performed between 20 and 85 °C. The samples were prepared in a drybox and kept in a strictly inert argon atmosphere throughout the measuring period. Conductivity was determined from complex impedance measurements using the "equivalent circuit" software package developed by Boukamp[21] and the equivalent circuit model reported in ref 14. The error in the resistance of the samples from the fit results was less than 3%.

Results and Discussion

Characterization of LiCl Preparations. It is well-known that metal halogen salts show high lattice energies, which increase as the atomic weight of halogen decreases.[12] Thus, in order to prepare polymer electrolytes using these types of salts it is necessary to dissolve both the salt and the polymer in a common solvent and then to eliminate the solvent by evaporation (solvent casting process).[1] As reported in several studies,[1,8,12] the properties of these materials are strongly affected by the solvent used in the preparation of the electrolytic complexes. In fact, it is very difficult to completely eliminate the solvent from the polymer electrolyte, and the solvent residue plays a determining role in the coordination process of the cation. In a previous study,[14] we completely resolved this problem by directly synthesizing an $MgCl_2$ salt having high crystallographic disorder and a low lattice energy. As reported, here this procedure also allowed us to obtain a very anhydrous lithium chloride salt that is very soluble in PEG 400. This material is produced by the following simple single-step reaction:

$$\text{Li(s)} + \text{1-chlorobutane(l)} \xrightarrow[\text{(b) } \Delta\text{. reflux}]{\text{(a) argon atmosphere}} \text{LiCl(s)} \quad (1)$$

The reaction is slower than that carried out using Mg[14] and must be performed in a stricly pure atmosphere of argon to avoid the formation of lithium oxide and nitride side products. Figure 1 reports the powder X-ray diffraction (XRD) spectra of the following lithium chloride samples: a commercial LiCl sample that was purified by treating the sample first with thionyl chloride and then under vacuum at 10^{-5} mbar for 1 week (Figure 1a); a sample obtained by reaction 1 (Figure 1b); a second

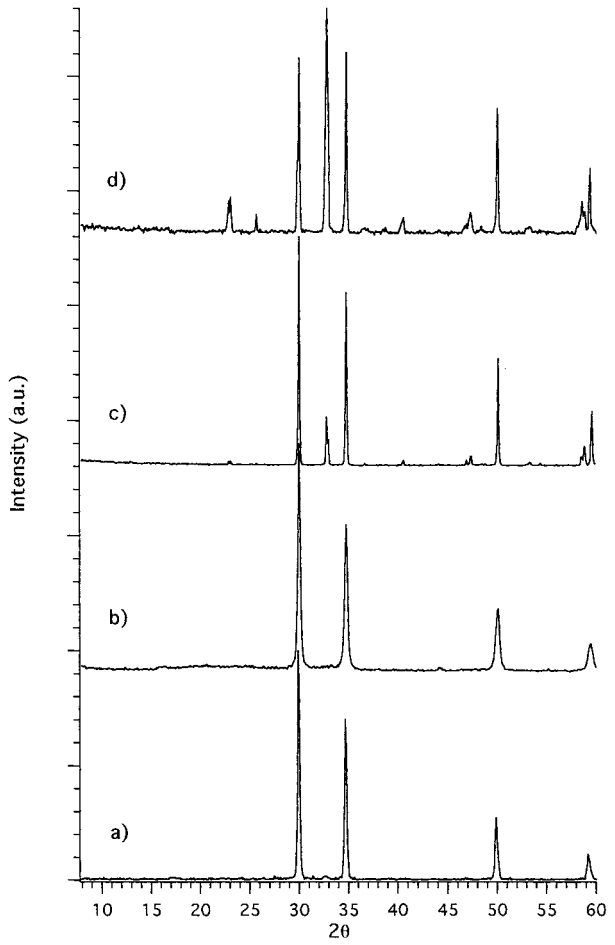

Figure 1. Powder X-ray diffraction patterns of LiCl samples: (a) commercial LiCl sample after purification with thionyl chloride and subsequent treatment under vacuum at 10^{-5} mbar for 1 week; (b) LiCl obtained by reaction 1; (c) LiCl obtained by reaction 1 after a low degree of hydration; (d) spectrum of hydrated commercial LiCl.

product obtained by reaction 1 with a low degree of hydration (Figure 1c); and a hydrated commercial LiCl (Figure 1d). In the spectra of Figure 1, c and d, the peaks at $2\theta = 30°$ and 34° are in agreement with those reported in the literature[22] and show intensities that differ from those observed for the samples of Figure 1, a and b. The other peaks in this spectral region correspond to a well-known crystallographic form of hydrated LiCl.[22] The spectra of Figure 1a,b are in agreement with the spectral data obtained earlier[23] for a highly anhydrous crystallographic form of LiCl in the space group $Fm\bar{3}m$. A comparison of the XRD spectra in Figure 1a,b evidences that LiCl obtained by reaction 1 is characterized by a comparatively high degree of crystallographic disorder. This observation suggests that the lattice energy of this material could be lower compared to that of LiCl obtained by rigorous purification of the commercial material. The far-IR spectra of the samples of Figure 1, b and c, are reported in Figure 2, a and b, respectively. The band peaking at 230 cm^{-1} is associated with the vibration ν(Li−Cl).[24] In the spectrum of partially hydrated LiCl (Figure 2b), the intensities observed at 330 and 384 cm^{-1} were attributed correlative to the vibrations ν(Li−O).[25,26]

These findings indicate that our very simple, single-step reaction yields a very pure LiCl preparation. Moreover, the salt is highly reactive toward Lewis bases, indicating that it possesses a low lattice energy. These properties makes it suitable for the preparation of very pure polymer electrolytes without the need for solvents.

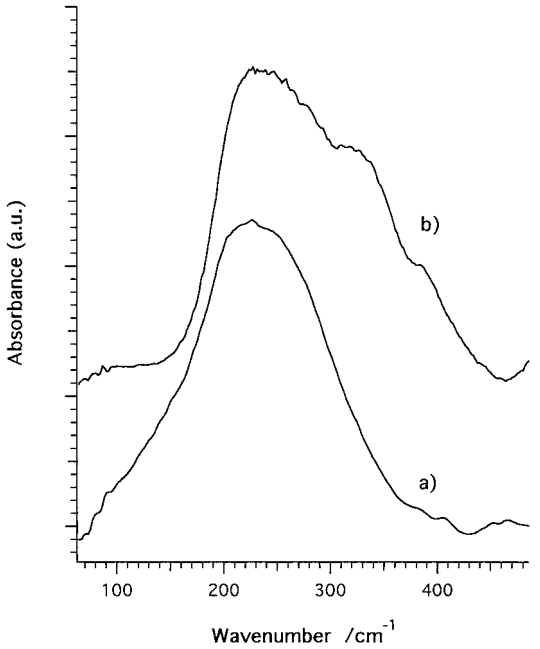

Figure 2. Far FT-IR absorption spectra of LiCl samples obtained by reaction 1: (a) anhydrous sample; (b) partially hydrated sample.

FT-IR Spectroscopy of PEG 400/$(LiCl)_x$ Complexes. Interactions between ions and PEG 400 in PEG 400/$(LiCl)_x$ polymer electrolytes were investigated by FT-IR spectroscopy. Unfortunately, it was not possible to obtain Raman spectra of the electrolytic complexes using the argon ion laser lines available in our laboratory because of the strong fluorescence interference induced by the dissolved salt.

The mid FT-IR spectra of PEG 400/$(LiCl)_x$ complexes with $0 \leq \times \leq 1.40665$ are depicted in Figure 3. In agreement with the literature,[11,14,27−29] these spectra were normalized with respect to the bands at 1294 and 1248 cm^{-1}, which represent vibrational modes that are not influenced by the conformational changes of the polyether chains. A detailed analysis of Figure 3 reveals that as the value for x in the PEG 400/$(LiCl)_x$ complexes increases, the frequencies and intensities of the stronger bands change significantly. To gain a detailed understanding of the interactions between PEG 400 chains and the salt, we initially studied the spectrum of PEG 400 dissolved in CCl_4. In fact, it is well-known[30] that the interactions between solute molecules are broken when a compound is dissolved at a low concentration in CCl_4; the spectrum of the solute measured under these conditions is usually called the "free" spectrum. Figure 4a,b report, the difference spectrum of PEG 400 dissolved in CCl_4 (i.e., the "free spectrum"; full line), together with that of pure PEG 400 (dashed line). The difference spectrum was obtained by subtracting the CCl_4 spectrum from that obtained for the PEG-CCl_4 solution. A comparison of the "free" and pure PEG 400 spectra shows that when PEG 400 is dissolved in CCl_4, the hydrogen bonds between PEG 400 molecules are broken and the ν(OH) bands shift to higher frequencies (Figure 4a). Moreover, the 900−1200 cm^{-1} spectral range is sharper and better resolved in the "free" PEG 400 spectrum compared to that of pure PEG 400. Thus, in a Gaussian spectral decomposition of this spectrum (see inset in Figure 4b), we were able to identify five vibrational modes in this region and detected that the bands peaking at lower frequencies are strongly influenced by the molecular environment. In agreement with our previous results,[9−11,14] the bands in the 1220−1330 cm^{-1} region are not influenced by intermolecular interactions.

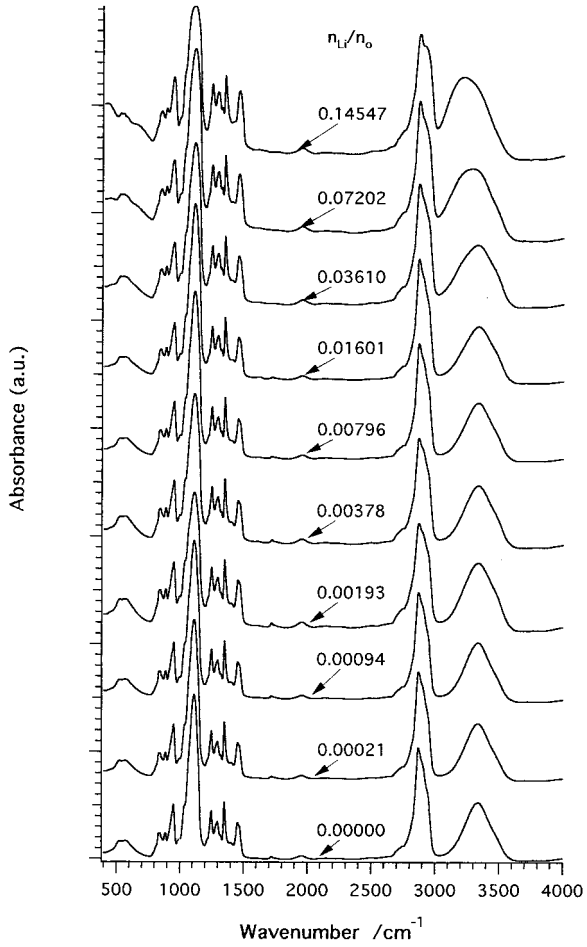

Figure 3. Mid FT-IR absorption spectra of PEG 400/$(LiCl)_x$ complexes. The Li/O molar ratios are indicated along the spectra.

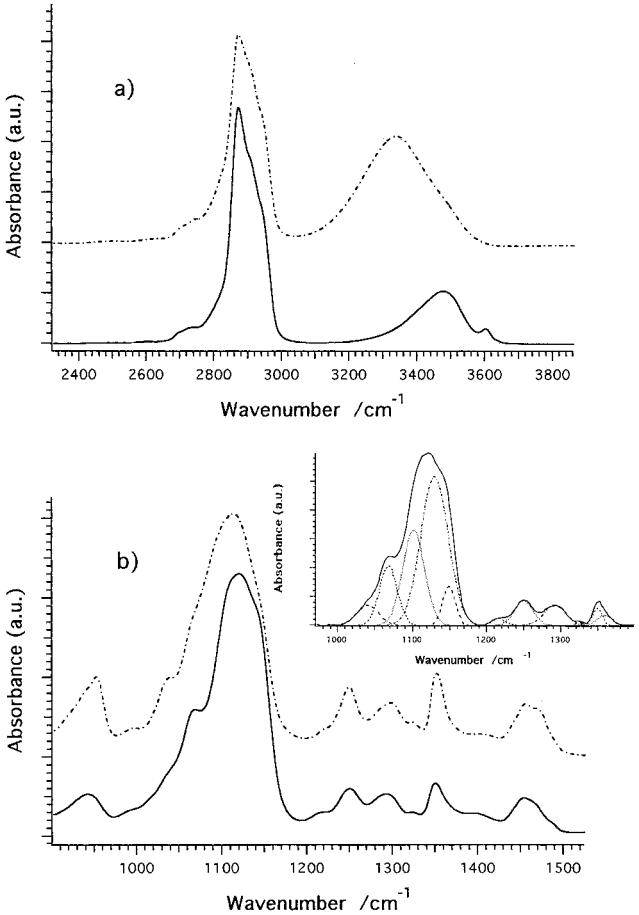

Figure 4. Spectrum of pure PEG 400 (dashed line) and difference spectrum of PEG 400 ("free spectrum") dissolved in CCl_4 (solid line). The difference spectrum was obtained by subtracting the CCl_4 spectrum from that of a solution of 0.056 g/mL of PEG 400 in CCl_4. (a) 3800−2400 cm^{-1} spectral region; (b) 1500−900 cm^{-1} spectral region. The inset reports the decomposition by Gaussian functions of the "free" PEG 400 spectrum.

In the spectrum of pure PEG 400, we attributed the bands peaking at 3494 and 3335 cm^{-1} to the vibrational modes ν^a(OH) and ν^s(OH), respectively.[31,32] In the spectrum of "free" PEG 400, these vibrational modes are observed at 3605 and 3480 cm^{-1}, respectively, thus indicating that the hydrogen bond structure of pure PEG 400 shifts the vibrations ν^a(OH) and ν^s(OH) to lower frequencies, by about 145 and 110 cm^{-1}, respectively. For aqueous solutions, it has been reported[33−35] that a decrease in the OH stretching frequency by 50 cm^{-1} corresponds to an increase in the hydrogen bond strength by roughly 1 kcal/mol. If this empirical rule is applied to the PEG 400 solutions, we can estimate the average hydrogen bond strength between PEG 400 molecules to be about 2.55 kcal/mol.

The band assignments of the spectra of pure PEG 400 and of PEG 400/$(LiCl)_x$ complexes with low x values were carried out correlatively on the basis of previous results[36−38] and of the normal coordinate treatment based on a TGT (T = trans; G = gauche) structural model of polyether chains under the factor group $D(4\pi/7)$.[36] The normal-coordinate analysis of polyether chains was performed by Miyazawa et al.,[37] who proposed that PEG chains assume a helical structure with internal rotation angles of $\tau(CH_2-CH_2) = 60°$ (gauche) and $\tau(O-CH_2) = \tau(CH_2-O) = 191.5°$ (trans). The correlative assignments of the spectral peaks are summarized in Table 2. Figure 5 reports the far FT-IR spectra of PEG 400/$(LiCl)_x$ complexes, which show that the deformation vibrations of PEG chains are located at the expected frequencies. It is to be noted that as the x value increases, the intensity of the bands peaking at 530 and 565 cm^{-1} decreases; these bands are assigned to the bending of CH_2-CH_2-O and rocking of CH_2 groups, respectively. The other polyether bands also present slight changes as x increases, and two new peaks arise at 370 and 427 cm^{-1}. A comparison of the spectra of Figure 5 with those of Figure 2 indicates that the Li−Cl vibrations are absent for a Li/O molar ratio (r) less than 0.036 and that the bands peaking at 370 and 427 cm^{-1} can be assigned with certainty to the vibrations ν(Li−O).[25,26] These modes are shifted to higher frequencies (by ca. 40 cm^{-1}) in the polymer electrolytes with respect to those of the partially hydrated sample of LiCl. Finally, we can conclude that the complexation of lithium ions by PEG oxygens is complete and that Li^+-Cl^- ion pairs are absent when $r < 0.036$. These results are in agreement with those obtained by Xu et al.[39] for poly(propylene oxide glycol)−400/$LiClO_4$ on the basis of audio frequency electrical conductivity measurements and infrared spectra of the ν_4 mode of ClO_4^-.

To better understand the nature of the LiCl−PEG 400 interactions, the bands in the mid FT-IR spectra exhibiting the highest intensities were investigated in depth. We focused particular attention on the 4000−2000 and 1700−700 cm^{-1} regions, where the peaks associated with the functional groups directly involved in the salt−polyether chain interactions are detected. Thus, the spectra were first corrected for background and then decomposed by Gaussian functions. Figures 6 and 7 report some of the decomposition results obtained for the 4000−2000 and 1700−700 cm^{-1} regions, respectively. The peaks

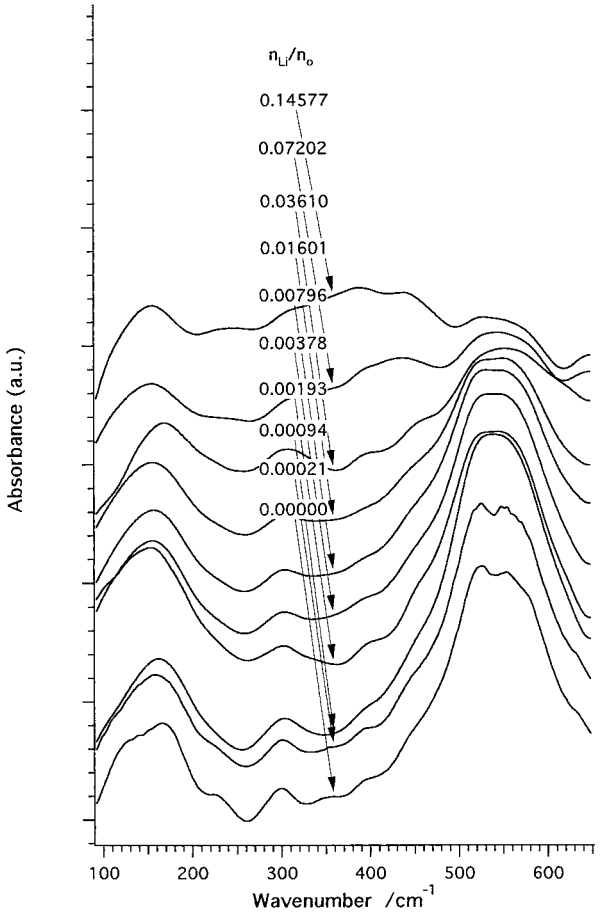

Figure 5. Far FT-IR absorption spectra of PEG 400/$(LiCl)_x$ complexes. The Li/O molar ratios are indicated along the spectra.

composing the bands in the 3100−3600 and 900−1200 cm^{-1} regions, which correspond to the ν(O−H) and ν(C−O) stretching vibrations, were decomposed as reported by Pelican et al.[40] by analyzing the properties of the first four derivatives of the spectra. The results were then compared with those obtained for the "free" PEG 400 spectrum. This analysis allowed us to discriminate three types of ν(O−H) vibrations in the 3200−3600 cm^{-1} region and five superimposed bands in the 900−1200 cm^{-1} region.

The band detected in the PEG 400/$(LiCl)_x$ complexes at ca. 3191 cm^{-1} (Figure 6) increases in intensity as the concentration of LiCl in the electrolytic complexes rises. On the basis of previous vibrational studies carried out on ethanolic and methanolic lithium chloride solutions,[41−43] this band was ascribed to the O−H stretching vibration of PEG 400 molecules hydrogen-bonded to chloride ions and weakly bonded to other PEG 400 molecules (see Scheme 1C). Scheme 1 summarizes the most probable interactions involving the −OH functional groups of PEG 400 molecules in "free" PEG 400 (A), pure PEG 400 (B), and electrolytic complexes (C), along with the approximate average values of the hydrogen-bonding strength determined as described above. In addition, a careful inspection of the spectra of Figure 7 shows that as x in the electrolytic complexes increases, significant changes are detected in the band intensities ascribed to the C−O and deformation vibrational modes of CH_2 occurring at 1360 and 1350 cm^{-1}. However, as expected, the bands peaking at 1294 and 1248 cm^{-1} appear to be insensitive to increases in salt concentration. To study the Li−PEG 400 interactions in greater details, the dependence of the band area ratios A_ν/A_R on the Li/O molar ratio (r) was analyzed. A_ν is the area of the peak at frequency ν and A_R that

SCHEME 1: Hydrogen-Bonded Structures Formed by Terminal Hydroxyl Groups of PEG 400 Molecules[a]

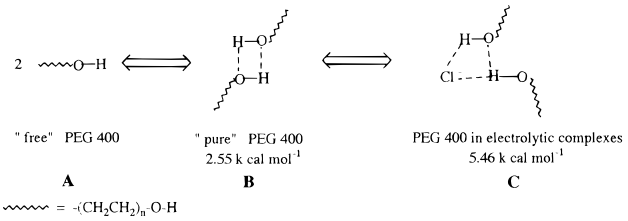

[a] (A) −OH groups not involved in hydrogen bonding; (B) possible hydrogen bonds between PEG 400 molecules; (C) probable orientation of solvent molecules bound to Cl^- ions.

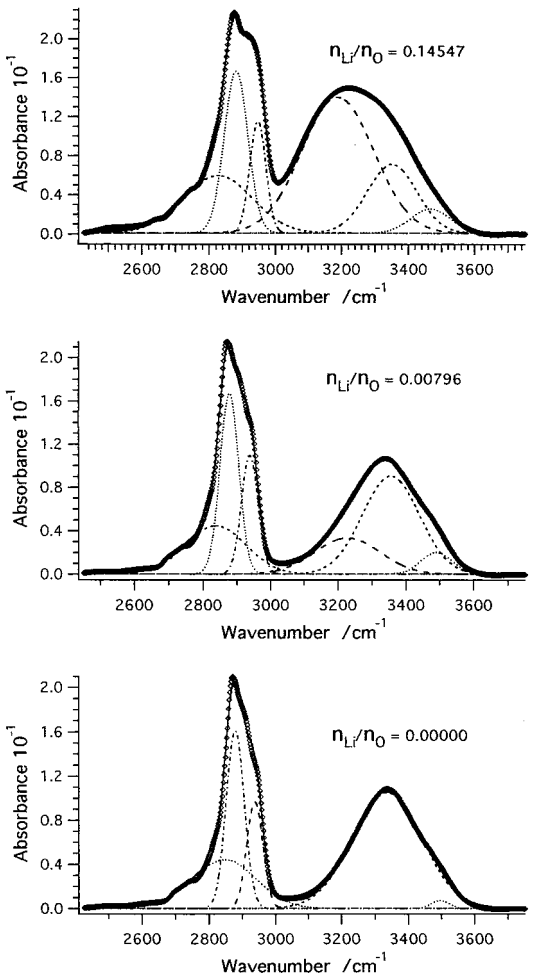

Figure 6. Decomposition by Gaussian functions of the mid FT-IR spectral range from 2500 to 3700 cm^{-1} of some selected PEG 400/$(LiCl)_x$ electrolytic complexes. The Li/O molar ratios are indicated in the spectra.

of the peak at 1294 cm^{-1}. Figure 8a shows that in the 2400−3700 cm^{-1} spectral range, as r rises, the intensity of the vibrational modes associated with the hydrogen-bonding structure also changes significantly. The intensity of the peaks attributed to the ν(OH) stretching of hydroxyls involved in hydrogen bonds between PEG 400 molecules (see Scheme 1B) decreases exponentially as r increases, while the intensity of the vibrational mode attributed to hydroxyl groups of PEG 400 molecules involved in hydrogen-bonding clusters of Cl^- ions (see Scheme 1C) increases as r rises. It is to be noted that these curves intersect at an Li/O molar ratio $\simeq$0.036.

Figure 8b reports a similar analysis carried out in the 1200−1400 cm^{-1} region. As reported in Table 2, this spectral region

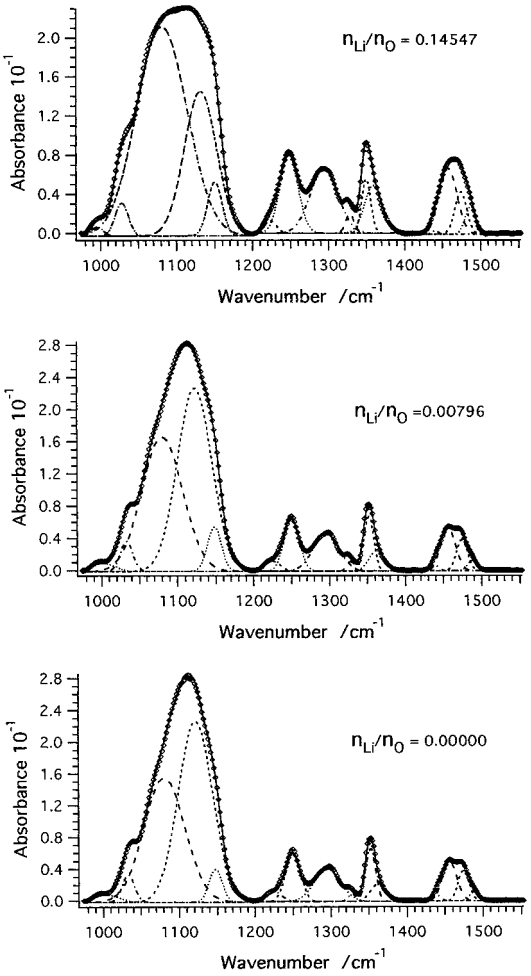

Figure 7. Decomposition by Gaussian functions of the mid FT-IR spectral range from 950 to 1550 cm^{-1} of some selected PEG 400/$(LiCl)_x$ electrolytic complexes. The Li/O molar ratios are indicated in the spectra.

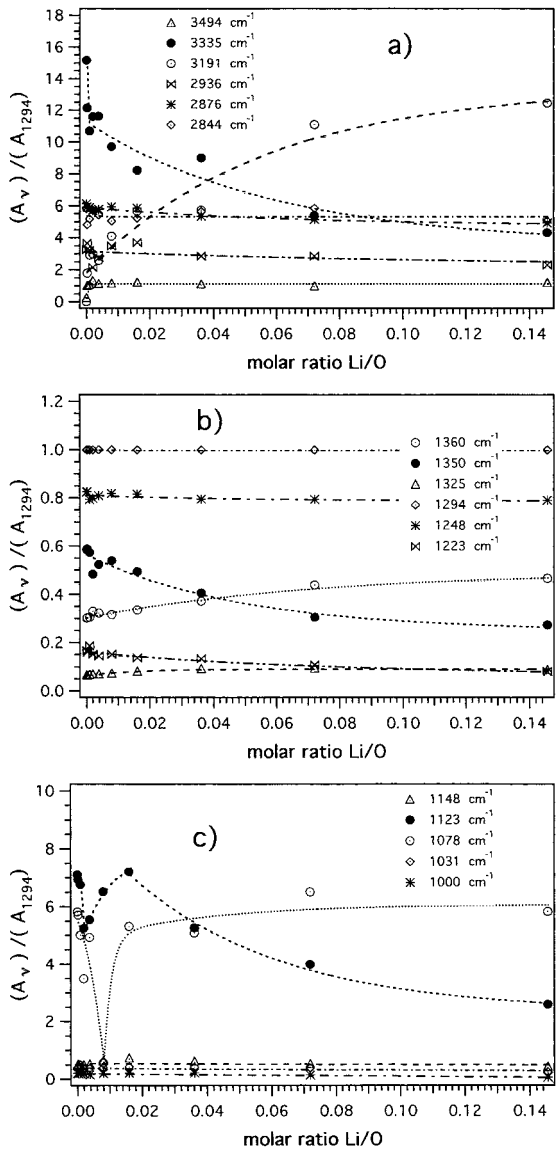

Figure 8. Relationship between A_ν/A_{1294} and the Li/O molar ratio in the PEG 400/$(LiCl)_x$ complexes. A_ν is the peak area at ν and A_{1294} is the area of the reference peak at 1294 cm^{-1}. (a) 2000−3700 cm^{-1} region; (b) 1300−1200 cm^{-1} region; (c) 900−1200 cm^{-1} region.

shows the bending vibrations of polyether chains and the w(CH_2) (A_2) and w(CH_2) (E_1) peaks at 1350 and 1360 cm^{-1}, respectively, which seems to be influenced by the salt concentration present in PEG 400/$(LiCl)_x$ complexes. It is noteworthy that as r rises, the profiles of the band peaking at 1360 cm^{-1} increases, while that at 1350 cm^{-1} decreases. These results demonstrate that as the salt concentration in the complexes increases, the distribution of torsion angles, $\tau(CH_2-CH_2)$, in PEG 400 chains could rearrange with respect to the starting value of 60° due to the gauche conformation. Therefore, we belive that as r increases, the average conformation distribution of polyether chains is slightly modulated. The intensities of the vibrational modes peaking at 1327−1223 cm^{-1} are weakly influenced by the salt concentration in the complexes. However, as observed above, the profiles of the curves peaking at 1360 and 1350 cm^{-1} intersect at an Li/O molar ratio ≃0.036.

On the basis of these findings, we propose that the conformation of the polyether chains in the complexes could be directly related to the hydrogen bond structures. Furthermore, variations in intensity ratio profiles versus r values are detected in the spectral region involving the C−O stretching modes (900−1200 cm^{-1}). In fact, as shown in Figure 8c, only two of these vibrational modes are significantly affected by the LiCl concentration in the host PEG 400. The first mode peaks at 1123 cm^{-1} and, after an increase in intensity in the $3 \times 10^{-3} \leq r \leq 1.8 \times 10^{-2}$ range, exhibits an exponential decrease. The second mode peaks at 1078 cm^{-1} and shows the opposite behavior. However, again, the curves intersect at an Li/O molar ratio ≃0.036.

These observations prompt us to hypothesize that, as r rises, two distinct phenomena could take place in the electrolytic complexes: (a) the hydrogen-bonding structure is gradually modified; and (b) the conformation of PEG 400 chains is modulated step by step to a very slight extent. To clarify these aspects in depth we investigated the effect of r on the vibrational frequencies of PEG 400 chains. Figure 9a shows that in the $0 \leq x \leq 1.40665$ range, ν(OH) vibrational modes show the following maximum frequency shifts: $\Delta\nu^a(OH) \simeq 29$ cm^{-1}; $\Delta\nu^s(OH) \simeq 32$ cm^{-1}; and $\Delta\nu^{Hy}(OH) \simeq 48$ cm^{-1}. $\Delta\nu^a(OH)$ shifts to lower frequencies, while $\Delta\nu^s(OH)$ and $\Delta\nu^{Hy}(OH)$ exhibit opposite behaviors. Now, one issue of nomenclature is necessary for sake of clarity when x is ranging in $0 \leq x \leq 1.40665$ values: (a) the vibrational modes with a frequency shift of $\Delta\nu \leq 8$ cm^{-1} can be considered insensitive to the environment of the macromolecule (η-type); (b) the frequencies presenting $8 < \Delta\nu \leq 20$ cm^{-1} can be considered weakly sensitive to the environment (ω-type); (c) the modes showing a shift ranging

TABLE 2: Molecular Vibration Assignments of the PEG 400/(LiCl)$_x$ Electrolytic Complexes under the *D* ($4\pi/7$) Symmetry Group

species	wavenumber (cm^{-1}) obsd[a]	wavenumber (cm^{-1}) calcd[b]	assignment and potential energy distribn[b,c]	ref
A_2	3494 (m)		ν^a(OH)	31, 32
	3335 (s) }		ν^s(OH)	31, 32
	3191 (s) }		ν^{Hy}(OH)	41−43
	2876 (s)	2883	ν^s(CH_2) (100)	36−38
	1473 (m) }	1470	sr(CH_2) (100)	36−38
	1455 (m) }			
	1350 (m) }	1344	w(CH_2) (107)	36−38
	1325 (vw) }			
	1248 (m)	1264	t(CH_2) (81)	36−38
	1078 (vs sh)	1087	ν(CO) (94)	36−38
	953 (m)	964	r(CH_2) (49), t(CH_2) (18)	36−38
	569 (w) }	533	δ(CCO) (89), r(CH_2) (33)	36−38
	548 (w) }			
	370 (vw)	340	ν^s(Li − O), ν_1(A_1)	25, 26
	230 (vw)		ν(Li−Cl)	24
E_1	2936 (sh)	2940	ν^a(CH_2), (101, 18°)	36−38
	2844 (vs)	2873	ν^s(CH_2), (100, −5°)	36−38
	1487 (w)	1471	sr(CH_2), (100, −132°)	36−38
	1439 (sh)	1401	w(CH_2), (95, 53°)	36−38
	1360 (sh)	1353	w(CH_2), (107, −129°)	36−38
	1294 (m)	1286	t(CH_2), (73, −40°)	36−38
	1223 (w)	1234	t(CH_2), (87, 116°)	36−38
	1148 (vw)	1142	ν(CO) (37, −27°), r(CH_2) (29, −66°)	36−38
	1123 (vs)	1112	ν(CO), (81, 136°), ν(C−C) (21)	36−38
	1031 (w)	1060	ν(CO) (36, −102°), r(CH_2) (35, 70°), ν(CC) (17)	36−38
	1000 (vw)	941	r(CH_2) (34, 42°), ν(CC) (27), ν(CO) (14, 167°)	36−38
	887 (w) }	847	r(CH_2) (58, −149°), ν(CO) (39, −9)	36−38
	845 (w) }			
	835 (w) }			
	525 (vw)	524	δ(CCO) (43, −142°), δ(COC) (21), r(CH_2) (17, 152°)	36−38
	427 (vw)	478 (?)	ν(Li−O), ν_3(B_1)	25, 26
	300 (w)	366	δ(CCO) (42, −73°), δ(COC) (38)	36−38
	160 (w)	164	ϕ_i(CC) (42), ϕ_i(CO) (38, −161°), δ(CCO) (18, 16°)	36−38

[a] Relative intensities are reported in parentheses; vs: very strong; s: strong; m: medium; w: weak; vw: very weak; sh: shoulder. [b] The normal-coordinate analysis was derived from the references reported in the last column. [c] ν, stretching; δ, bending; w, wagging; t, twisting; r, rocking; sr, scissoring; ϕ_i, internal rotation; a, antisymmetric mode; s, symmetric mode.

from $20 < \Delta\nu \leq 30$ cm^{-1} can be considered as affected to a moderate extent by the doping salt concentration (μ-type); (d) the frequencies shifted by $30 < \Delta\nu \leq 40$ cm^{-1} are due to modes strongly affected by the salt concentration (σ-type); and (e) those exhibiting $\Delta\nu > 40$ cm^{-1} can be considered very strongly affected by the ion-macromolecule interaction (vσ-type). Therefore, the modes reported in Figure 9a can be classified as $\nu^{Hy}_{v\sigma}$(OH), ν^s_σ(OH) and ν^a_μ(OH), respectively, indicating that the first two vibrations are strongly diagnostic in studies of salt−polyether chain interactions. Furthermore, the C−H stretching modes detected in the 2820−2960 cm^{-1} region and the bending vibrations peaking from 1220 to 1500 cm^{-1} are identified as η-type vibrations, which are insensitive to the environment and demonstrate that the conformation of PEG 400 chains in the electrolytic systems is modified very slightly by the LiCl concentration. Figure 9b illustrates that in the 1000−1200 cm^{-1} region, the frequencies associated with the C−O vibration components (see Table 2) are all of the ω-type, except for the band peaking at ca. 1148 cm^{-1} (E_1), which is η-type. These ω-type vibrations can be classified into two distinct groups: the first group is constituted by the frequencies at ca. 1031 (E_1) and 1000 (E_1) cm^{-1}, which decrease as x increases; the second group exhibits the opposite behavior and is composed of the frequencies at ca. 1078 (A_2) and 1123 (E_1) cm^{-1}. These observations prompt us to consider these vibrational modes as diagnostic vibrations for the salt−polyether chain complexation process. In fact, in agreement with the literature,[44−46] the modulation of the frequencies ascribed to the vibrational modes

SCHEME 2: Electron Shift in PEG C−O Bonds[a]

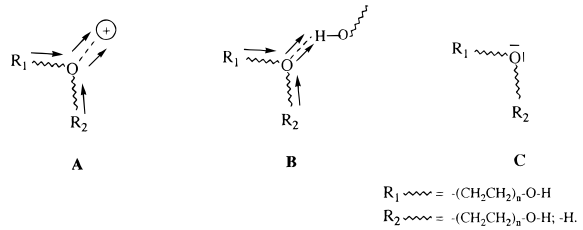

[a] (A) PEG oxygens coordinating a cation; (B) PEG oxygens involved in hydrogen bonding between PEG 400 molecules; (C) "free" PEG 400 molecules.

involving C−O bonds can be correlated to the lithium cation coordination. It was proposed that the electron shift toward the oxygen atom in the C−O bond is associated with a decrease in the frequency and an increase in the intensity of the C−O stretching vibration with respect to those observed in the "free" ligand.[44−45] On the other hand, the electron shift in the opposite direction is associated with an increase in the frequency and a decrease in the intensity compared with "free" ligand. Now, if we consider that the interaction of an electron acceptor species or a cation with the oxygen atom causes a decrease in the frequency and an increase in intensity of the C−O stretching band (Scheme 2 A and B), we can recognize that the breaking of hydrogen bonds (Scheme 2B), leads to an increase in the frequency and a decrease in the intensity of the C−O frequency stretching band. In conclusion, the results depicted in Figures 8c and 9b suggest that as x in the PEG 400/(LiCl)$_x$ complexes

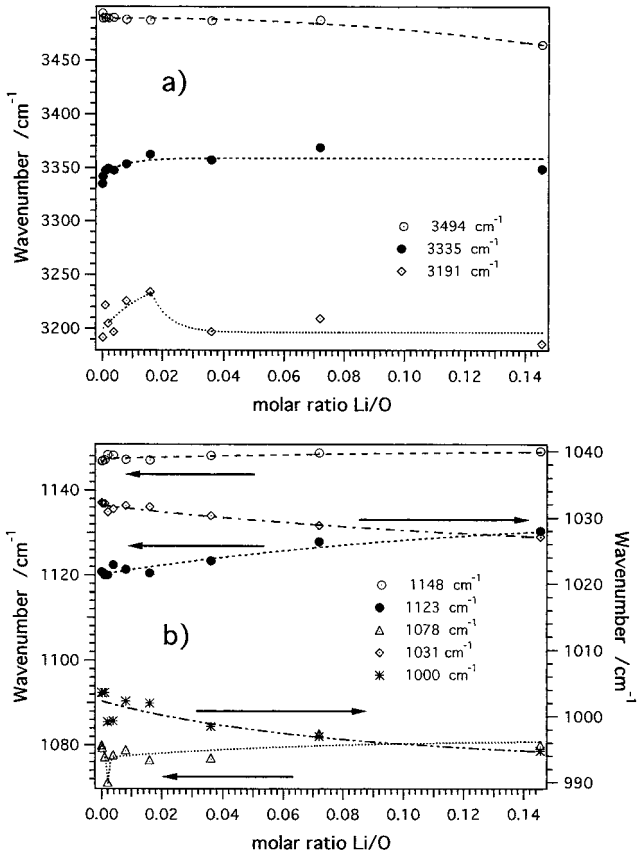

Figure 9. Effect of Li/O molar ratio in PEG 400/$(LiCl)_x$ complexes on the vibrational frequencies: (a) 3000−3700 cm^{-1} region; (b) 1200−950 cm^{-1} region.

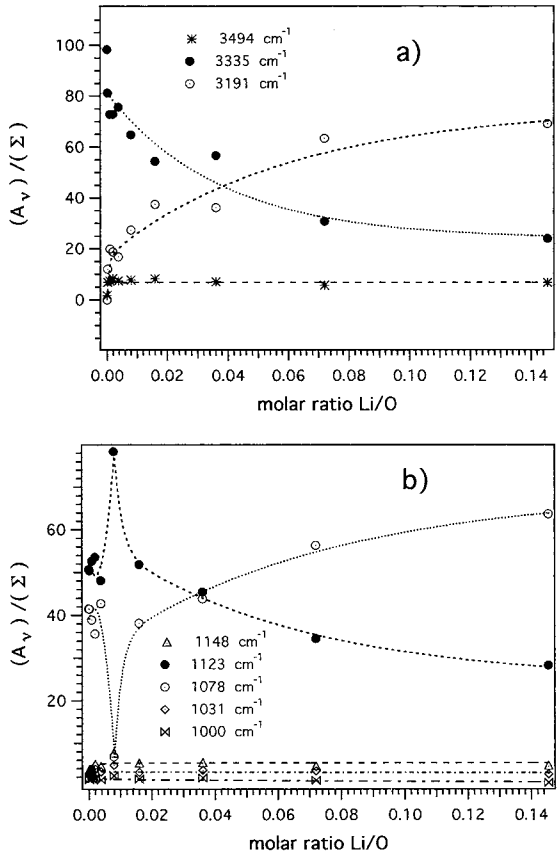

Figure 10. Relationship between $A\nu/\Sigma$ and the Li/O molar ratio in PEG 400/$(LiCl)_x$ complexes. A_ν is the peak area at ν and $\Sigma = \sum_{i=1}^{n} A_\nu$ is the sum of n band areas of the vibrations attributed to a particular functional group. (a) 3000−3700 cm^{-1} region; (b) 1200−950 cm^{-1} region.

increases, two phenomena take place: (a) the concentration of oxygen atoms in PEG 400 chains that are coordinated to Li^+ increases, thereby giving rise to a decrease in the frequency and an increase in the intensity of the bands peaking at 1031 and 1000 cm^{-1} (also see Scheme 2A); (b) the concentration of hydrogen-bonded structures depicted in Scheme 2B decreases, giving rise to an increase in the frequency and a decrease in the intensity of the involved bands (see band peaking at 1123 cm^{-1} and Figures 9b and 8c).

Finally, we can conclude that as x increases, the mode diagnostic for the formation or breaking of hydrogen bonds between PEG 400 molecules is found at 1123 cm^{-1}, which, as reported in Table 2, is attributed to a mode having a high C−O stretching contribution, ν(CO)(81,136°),ν(C−C)(21). The vibrations diagnostic for the coordination of Li^+ cations peak at 1031 and 1000 cm^{-1}, which are modes due to ν(CO) stretching combined with $r(CH_2)$ and ν(C−C) vibrations (see Table 2). Moreover, the intensity peaking at 1078 cm^{-1} appears to be anomalous and dependent on the x value. This mode increases in both intensity and frequency as x rises (see Figures 8c and 9b) and was assigned totally to the ν(C−O) stretching vibration in the spectrum of pure PEG 400 molecules. We attribute this vibration to the terminal C−O groups of PEG 400 molecules, which, as depicted in Scheme 1C, are influenced by the anion coordination. In fact, in this case, as x increases, electrons shift back from oxygen to the carbon atom of the C−O bond, thus increasing both the frequency and the intensity of the band.[44−46]

The effect of x on the hydrogen-bond structures formed in the electrolytic complexes was studied in more detail by analyzing the band absorbances in the 3100−3600 and 900−1200 cm^{-1} regions, which are associated with the ν(OH) and ν(CO) stretching vibrations, respectively.

A semiquantitative measure of the fractional amount of each type of OH and CO group in the electrolytic complexes was obtained by determining the ratio $R_\nu = A_\nu/\Sigma$, where A_ν is the band area contributed by a definite type of functional group absorbing at ν, and Σ is the sum of all the band areas of the modes contributed by a particular functional group. Figure 10a reports the relationship between r and the percentages of each type of OH group present in the electrolytic complexes. It is to be noted that as r increases, the concentration of hydroxyl groups involved in the hydrogen-bonding structure formed between PEG 400 molecules and Cl^- ions (Scheme 1C) rises, while those corresponding to the hydrogen bonding structure between PEG 400 molecules decreases (Scheme 1B). For $9 \times 10^{-3} \leq r \leq 0.15$, the bands peaking at 1123 and 1078 cm^{-1} (Figure 10b) can be superimposed on those reported in Figure 10a and intersect at an r value of ca. 0.036. This coincidence supports the assignment reported above and demonstrates that, for $9 \times 10^{-3} \leq r \leq 0.15$ the peak at 1078 cm^{-1} presents the same behavior as the band peaking at 3191 cm^{-1}, which is attributed to the terminal hydroxyl groups of PEG 400 macromolecules involved in the hydrogen-bonding structure of Cl^- ions. In this range of r values, the bands peaking at 3335 and 1123 cm^{-1} present similar profiles, thus indicating that these vibrational modes are related to physical events associated with the same hydrogen-bonding structure (Scheme 1B).

The average number of OH terminal groups (ψ) participating in the Cl^- hydrogen-bonding cages can be calculated as $\psi = (2R_{OH_b}/100)n_{PEG}/n_{Cl^-}$, where $R_{OH_b} = R_{3207}$ is the percentage of OH terminal groups involved in Cl^- hydrogen-bonding cages, n_{PEG} is the number of moles of PEG 400 molecules and n_{Cl^-}

the moles of Cl^- present in the electrolytic complexes. The dependence of ψ on the Li/O molar ratio (r) is reported in Figure 11 a. It is to be observed that $r \simeq 0.036$ corresponds to $\psi \simeq 4$, indicating that a tetrahedral coordination geometry around Cl^- ions is to be expected at this r value.

Let us assume that, for a given x value, the following equilibrium takes place in the PEG 400/$(LiCl)_x$ complexes

$$\psi OH_{PEG} + Cl^- \leftrightarrow [Cl(OH)_\psi]^- \quad (2)$$

where OH_{PEG} represents the PEG 400 terminal hydroxyls that do not take part in Cl^- hydrogen-bonding cages, and $[Cl(OH)_\psi]^-$ represents the hydrogen-bonding clusters of chloride anions. Thus, the equilibrium constant of eq 2 can be written

$$K = \frac{R_{[Cl(OH)_\psi]^-}}{R^\psi_{OH_{PEG}} R_{Cl}} = \frac{R_{OH_b}}{\psi R^\psi_{OH_{PEG}} R_{Cl}} \quad (3)$$

where

$$R_{[Cl(OH)_\psi]^-} = (1/\psi) R_{OH_b} = \left[\frac{n_{[Cl(OH)_\psi]^-}}{n^T_{OH_{PEG}}}\right] \times 100$$

$$R_{OH_{PEG}} = \frac{n_{OH_{PEG}}}{n^T_{OH_{PEG}}} \times 100$$

$$R_{Cl} = \frac{n_{Cl}}{n^T_{OH_{PEG}}} \times 100$$

where $n_{[Cl(OH)_\psi]^-}$ is the number of moles of Cl^- hydrogen-bonding clusters formed by PEG OH groups, $n^T_{OH_{PEG}}$ is the total number of moles of hydroxyl groups present in the electrolytic complexes, $n_{OH_{PEG}}$ is the number of moles of terminal OH groups of PEG molecules not involved in the formation of Cl^- hydrogen-bonding clusters, and n_{Cl} is the moles of free Cl^- ions.

The dependence of KR_{Cl} on the Li/O molar ratio is reported in Figure 11b. It should be noted that electrolytic complexes with r values lower than 0.036 exhibit very low KR_{Cl} values. In fact, under these conditions, all of the Cl^- ions present in the electrolytic complexes are bonded by OH groups of PEG, thus forming hydrogen-bonding clusters. However, the concentration of "free" Cl^- ions (not participating in hydrogen-bonding clusters) rises monotonically when r is greater than 0.036.

Finally, these vibrational studies of PEG 400/$(LiCl)_x$ complexes allow us to conclude the following: (a) for $r \leq 0.036$, Li^+ ions are coordinated by the polyether oxygens of PEG chains, while Cl^- preferentially form hydrogen-bonding clusters with the terminal OH groups; (b) when $r > 0.036$, Li^+ is once more totally coordinated by polyether oxygens, and two different groups of Cl^- anions are present in the material. The first group represents Cl^- ions bound in the hydrogen-bonding clusters and the second group, which we call " free anions", are distributed along the PEG chains, thus dynamically satisfying the electroneutrality of the Li−PEG 400 complexes. Moreover, the far FT-IR spectra (Figure 5) of the electrolytic complexes at $r \geq 0.036$ show a very weak band at $\simeq$230 cm^{-1}. The presence of this band, which was attributed to the ν(Li−Cl) vibration (Table 2), indicates that a fraction of the "free anions" in the material are certainly implicated in the formation of Li···Cl ionic couples.

Conductivity Measurements. Figure 12 presents a plot of the conductivity of PEG 400/$(LiCl)_x$ systems for $0 \leq x \leq 1.40665$. The conductivity of these products increases monotonically as T rises. At 25 °C, PEG 400/$(LiCl)_{0.349}$ exhibits a conductivity of $\approx 1 \times 10^{-4}$ S cm^{-1}, which is approximately 1 order of magnitude higher than that observed for other highly conducting low molecular weight polymer electrolytes, such as PEG 400/$(MgCl_2)_x$,[14] PEG 800/LiCl,[47] etc. Furthermore, the conductivity data were fitted satisfactorily by the empirical Vogel−Tamman-Fulcher (VTF) type equation[1,8]

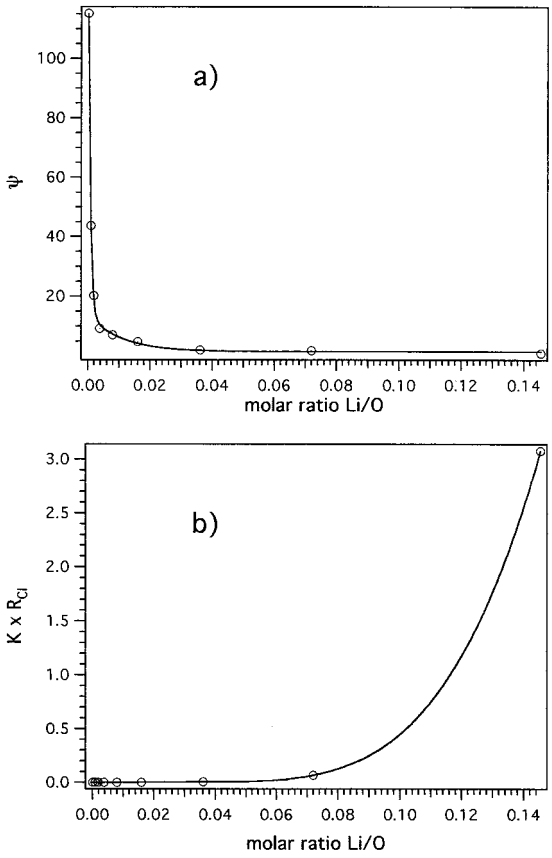

Figure 11. (a) Dependence of ψ on the Li/O molar ratio in PEG 400/$(LiCl)_x$ electrolytic complexes. ψ is the average number of OH terminal groups forming Cl^- hydrogen-bonding cages. (b) Dependence of KR_{Cl} on Li/O molar ratio in PEG 400/$(LiCl)_x$ complexes. K is the equilibrium constant between "free" terminal hydroxyls of PEG 400 and those participating in the Cl^- hydrogen-bonding structures. R_{Cl} is the fraction of "free anion" concentration.

$$\sigma(T) = A_\sigma T^{-1/2} e^{-E_a/k_b(T-T_0)} \quad (4)$$

where A_σ is proportional to the number of carrier ions, k_b is the Boltzmann constant, E_a is a constant that is related to the apparent activation energy, and T_0 is the thermodynamic ideal glass transition temperature at which the configurational entropy becomes zero or the "free" volume disappears. These parameters were determined by fitting eq 4 to the data in Figure 12. The fitting was carried out by assuming a starting T_0 value on the basis of the boundary condition[11] $(T_g - 55) \leq T_0 \leq (T_g - 40)$ and $T_g \simeq -60$ °C. These assumptions were taken in accordance with the common literature, which states that T_0 is normally found 50 K below T_g[15] in polymer electrolytes. Figure 13, a and b, report the dependence of final fitted values of E_a, T_0 and A_σ on the Li/O molar ratio.

It is to be noted that as the salt concentration increases, E_a rises and T_0 decreases monotonically (Figure 13a). We believe that this reflects the formation of extended dynamic PEG−salt−PEG cross-links at higher r values, which reduces the crystallinity and raises the activation energy of the system. Figure 13b

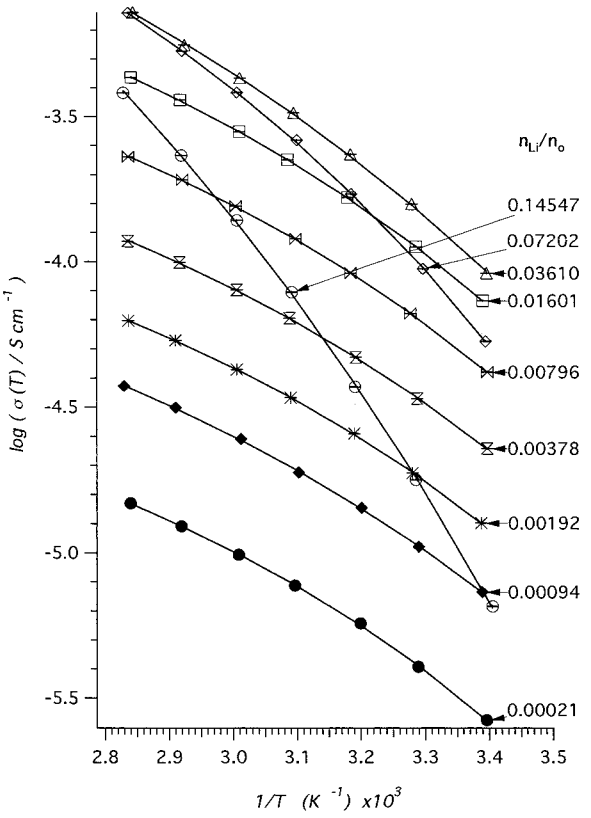

Figure 12. Plot of log(ionic conductivity) vs $1/T$ for PEG 400/$(LiCl)_x$ electrolytic complexes. The Li/O molar ratios are indicated in the plot.

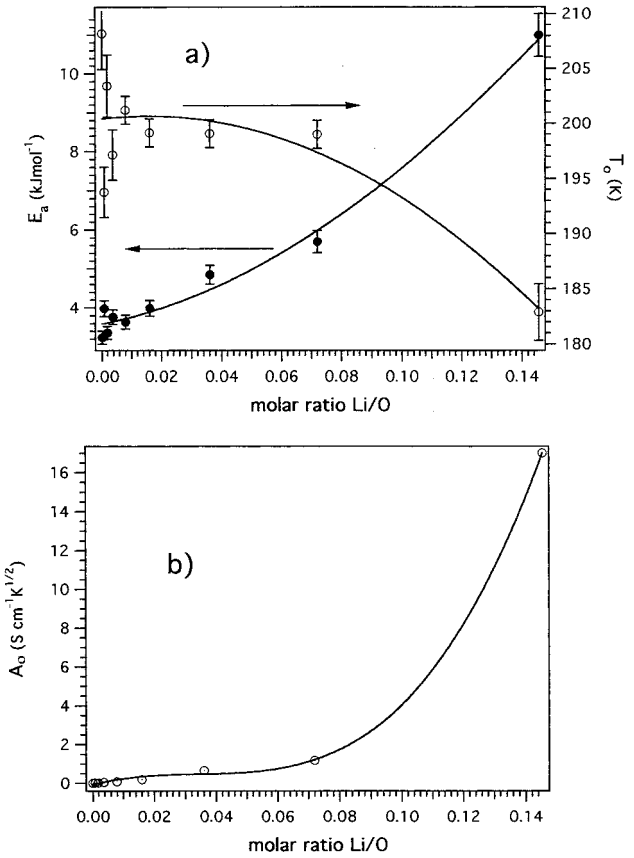

Figure 13. Dependence of VTF parameters on the Li/O molar ratio in PEG 400/$(LiCl)_x$ complexes: (a) T_0 and E_a; (b) preexponential factor A_σ.

presents a plot of A_σ versus the Li/O molar ratio. It can be seen that A_σ, which depends on the concentration of free ionic carriers, does not change significantly for Li/O molar ratios less than 0.036, but increases markedly when Li/O exceeds this value. This behavior is in agreement with our previous results obtained with PEG 400/$(EuCl_3)_x$[10] and PEG 400/$(MgCl_2)_x$,[14] and with the investigations carried out by Albinson et al. on the PPG 4000/$(LiCF_3SO_3)_x$[48] system. In conclusion, these data indicate that the concentration of "free ionic carriers" is very low for Li/O molar ratios less than 0.036 and increases exponentially for higher Li/O molar ratios.

Finally, a comparison of Figures 13b and 11b reveals that the profiles of A_σ and KR_{Cl} versus the Li/O molar ratio are very similar. This observation suggests that the "free ionic carriers", which are responsible for the A_σ values, are directly related to the total "free anion" concentration. These Cl^- ions are not involved in the hydrogen bonds formed by PEG chain terminal hydroxyls and instead are distributed along the PEG chains. This picture takes into account that in the electrolytic complexes with a Li/O molar ratio greater than 0.036, all the potential hydrogen-bonding sites are occupied, with the residual anion concentration engaged in dynamic PEG−salt−PEG cross-links. Furthermore, the existence of this type of interchain cross-link, which involves only ethereal oxygens of PEG chains and both the cation and the anion of the LiCl salt, could be responsible for the increase in the activation energy of the ion-hopping process and the reduced crystallinity of the samples.

Conclusions

A very reactive and extremely anhydrous LiCl salt was prepared by reacting powdered metallic lithium and 1-chlorobutane. PEG 400/$(LiCl)_x$ complexes with $0 \leq x \leq 1.40665$ were synthesized simply by direct dissolution of the anhydrous LiCl in PEG 400. The extremely anhydrous, solvent-free polymer electrolytes thus obtained allowed us to carry out very accurate FT-IR measurements in mid and far infrared.

FT-IR studies of these compounds disclosed the following structural properties: (a) the PEG chains exhibit a TGT type conformation; (b) the doping of PEG 400 with LiCl substantially modifies the hydrogen-bonding structures of the starting material but has an insignificant effect on chain conformation; (c) Li^+ ions are coordinated by the ethereal oxygen ligands of PEG 400; (d) at an Li/O molar ratio (r) less than 0.036, all Cl^- anions participate in hydrogen-bonding clusters with terminal hydroxyls of PEG chains; (e) when $r > 0.036$, Cl^- ions are preferentially involved in hydrogen-bonding clusters with terminal hydroxyls of PEG chains, with the remaining fraction of the total Cl^- ion concentration distributed along the PEG 400 chains, giving rise to the so-called "free anion" concentration. A portion of the "free anions" in the material are involved in the formation of Li−Cl ionic couples.

Conductivity results have been obtained for PEG 400/$(LiCl)_x$ complexes over the range of concentrations investigated. The conductivity data obtained are 1 order of magnitude higher than those determined for other analogous electrolytic systems containing alkali and alkaline earth salts. In particular, for the PEG 400/$(LiCl)_{0.345}$ complex at 25 °C a conductivity of $\simeq 1 \times 10^{-4}$ S cm^{-1} was observed. In addition, the conductivity data were fitted satisfactorily by the empirical VTF equation and distinguished two distinct types of electrolytic regions depending on the composition of the system. The first conductivity region is observed for the electrolytic systems with $r < 0.036$ and the second for those with $r > 0.036$. Moreover, our analysis demonstrates for the first time that the profile of A_σ versus r is strongly correlated with the equilibrium constant K and with

R_{Cl}, where K is the equilibrium constant between free terminal hydroxyls of PEG chains and those participating in the Cl^- hydrogen-bonding structures and R_{Cl} is the fraction of the "free anion" concentration. These findings allow us to conclude that the conductivity in the PEG 400/$(LiCl)_x$ complexes is ionic and, depending on the Li/O molar ratio, occurs by two different types of mechanisms. In particular, we hypothesize that for $r \leq 0.036$, the Cl^- ions are totally engaged in hydrogen-bonding cages and that Li^+ are coordinated by ethereal oxygens of PEG chains, thus giving rise to a cation-hopping process through adjacent sites along the PEG chains having equivalent coordination symmetry (pseudo-intra-CH mechanism). For $r > 0.036$ the increase in "free anion" concentration gives rise to further PEG−salt−PEG interactions which reduce the molecular mobility of the oligomer chains in the system and most likely contribute to inter-CH hopping, a phenomenon that substantially increases the preexponential factor in the VTF equation and explains the increase in the activation energy of the ion-hopping process.

It is clear that, below the entanglement molecular weight,[19] mobility of the polymer host is a determining factor in the inter-CH and intra-CH hopping mechanisms. However, as shown by the slopes of the conductivity versus temperature plots, the oligomer motion strongly influences the electrolytic systems that undergo inter-CH hopping (i.e., when $r \geq 0.036$).

Acknowledgment. The authors express their gratitude to Prof. R. Zannetti and Prof. A. Marigo for the use of their facilities for the powder XRD measurements.

References and Notes

(1) Gray, F. M. *Polymer Electrolytes, RSC Materials Monographs*; Royal Society of Chemistry: Cambridge, UK, 1997.
(2) Owen, J. *Chem. Soc. Rev.* **1997**, *26*, 259.
(3) Scrosati, B.; Neat, R. J. In *Applications of Electroactive Polymers*; Scrosati, B., Ed.; Chapman and Hall: London, 1993; p 182.
(4) Murata, K. *Electrochim. Acta* **1995**, *40*, 2177.
(5) Wright, P. V. *Electrochim. Acta* **1998**, *43*, 1137.
(6) Armand, M. *Adv. Mater.* **1990**, *2*, 278.
(7) Vaia, R. A.; Vasudevan, S.; Krawiec, W.; Scaulon, L. G.; Giannelis, E. P. *Adv. Mater.* **1995**, *7*, 155.
(8) Bruce, P. G.; Vincent, C. A. *J. Chem. Soc., Faraday Trans.* **1993**, *89*, 3187.
(9) Di Noto, V.; Bettinelli, M.; Furlani, M.; Lavina, S.; Vidali, M. *Macromol. Chem. Phys.* **1996**, *197*, 375.
(10) Di Noto, V.; Furlani, M.; Lavina, S. *Polym. Adv. Technol.* **1996**, *7*, 759.
(11) Di Noto, V. *J. Mater. Res.* **1997**, *12*, 3393.
(12) Ratner, M.; Shriver, D. F. *Chem. Rev.* **1988**, *88*, 109.
(13) Nowinski, J. L.; Lightfoot, P.; Bruce, P. G. *J. Mater. Chem.* **1994**, *4*, 1579.
(14) Di Noto, V.; Lavina, S.; Longo, D.; Vidali, M. *Electrochim. Acta* **1998**, *43*, 1225.
(15) Ratner, M. In *Polymer Electrolyte Rewiews-1*; McCallum, J. R., Vincent, C. A., Eds; Elsevier Applied Science: New York, 1989; Chapter 7.
(16) Ratner, M.; Nitzan, A. *Faraday Discuss. Chem. Soc.* **1989**, *88*, 19.
(17) Frech, R.; Chintapalli, S.; Bruce, P. G.; Vincent, C. A. *J. Chem. Soc., Chem. Commun.* **1997**, 157.
(18) Latham, R. J.; Linford, R. G. *Solid State Ionics* **1996**, *85*, 193.
(19) Ward, I. M.; Boden, N.; Cruickshank, J.; Leng, S. A. *Electrochim. Acta* **1995**, *40*, 2071.
(20) Di Noto, V.; Saccon, M.; Bresadola, S.; Zannetti, R. *Analyst (London)* **1990**, *115*, 1041.
(21) Boukamp, B. A. *Equivalent Circuit* (EQUIVCRT. PAS); Department of Chemical Technology, University of Twente, PO Box 217, 7500 AE Enschede, The Netherlands, 1989.
(22) Weiss, E.; Hensel, H.; Kühr, H. *Chem. Ber.* **1969**, *102*, 632.
(23) 22-1142 card from PDF-2 sets 1-42 database: Berry, W. L., Ed. Joint Committee on Powder Diffraction Standard (JCPDS-ICDD), 1601 Park Lane, Swarthmore, PA 19081, 1992.
(24) Adams, D. M. *Metal−Ligand and Related Vibrations*; Edward A., London, 1967, Chapter 2.
(25) Seshadri, K. S.; White, D.; Mann, D. E. *J. Chem. Phys.* **1966**, *45*, 4697.
(26) White, D.; Seshadri, K. S.; Dever, D. F.; Mann, D. E.; Linevsky, M. J. *J. Chem. Phys.* **1963**, *39*, 2463.
(27) Miyake, A. *J. Am. Chem. Soc.* **1960**, *82*, 3040.
(28) Kuroda, Y.; Kubo, M. *J. Polym. Sci.* **1959**, *36*, 453.
(29) Machida, K.; Miyazawa, T. *Spectrochim. Acta* **1964**, *20*, 1865.
(30) Hester, R. E.; Plane, R. A. *Spectrochim. Acta* **1967**, *23A*, 2289.
(31) Liddel, U.; Becker, E. D. *Spectrochim. Acta* **1957**, *10*, 70.
(32) Vien, D. L.; Colthup, N. B.; Fateley, W. G.; Grasselli, J. G. *The Handbook of Infrared and Raman Characteristic Frequencies of Organic Molecules*, Academic Press: Boston, 1991.
(33) Joesten, M. D.; Drago, R. S. *J. Am. Chem. Soc.* **1962**, *84*, 3817.
(34) Drago, R. S.; O'Bryan, N.; Vogel, G. C. *J. Am. Chem. Soc.* **1970**, *92*, 3924.
(35) Kanno, H.; Hiraishi, J. *J. Raman Spectrosc.* **1987**, *18*, 157.
(36) Matsuura, H.; Miyazawa, T. *Bull. Chem. Soc. Jpn.* **1968**, *41*, 1798.
(37) Miyazawa, T.; Fukushima, K.; Ideguchi, Y. *J. Chem. Phys.* **1962**, *37*, 2764.
(38) Yoshihara, T.; Tadokoro, H.; Murahashi, S. *J. Chem. Phys.* **1964**, *41*, 2902.
(39) Xu, M.; Eyring, E. M.; Petrucci, S. *J. Chem. Soc., Faraday Trans.* **1996**, *92*, 4969.
(40) Pelican, P.; Ceppan, M.; Lisko, M. *Application of Numerical Methods in Molecular Spectroscopy*; CRC Press: London, 1994; p 25.
(41) Yamauchi, S.; Kanno, H. *Chem. Phys. Lett.* **1989**, *154*, 248.
(42) Yamauchi, S.; Kanno, H. *J. Phys. Chem.* **1990**, *94*, 6594.
(43) Kanno, H.; Honshoh, M.; Yamauchi, S. *Z. Naturforsch.* **1995**, *50a*, 257.
(44) Kecki, Z. *Spectrochim. Acta* **1962**, *18*, 1155.
(45) Kecki, Z. *Spectrochim. Acta* **1962**, *18*, 1165.
(46) Kurowski, S.; Minc, S. *Spectrochim. Acta* **1963**, *19*, 345.
(47) Gupta, S.; Shahi, K.; Binesh, N.; Bhat, S. V. *Solid State Ionics* **1993**, *67*, 97.
(48) Albinsson, I.; Mellander, B.-E.; Stevens, J. R. *J. Chem. Phys.* **1992**, *96*, 681.